Eur. Phys. J. Plus (2017) **132**: 101
DOI 10.1140/epjp/i2017-11338-7

THE EUROPEAN PHYSICAL JOURNAL PLUS

Regular Article

Stefan blowing effects on MHD bioconvection flow of a nanofluid in the presence of gyrotactic microorganisms with active and passive nanoparticles flux

Shib Sankar Giri[1,a], Kalidas Das[2,b], and Prabir Kumar Kundu[3,c]

[1] Dept. of Basic Science, MCKV Institute of Engineering, Howrah-711204, West Bengal, India
[2] Dept. of Mathematics, A.B.N.Seal College, Cooch Behar, PIN-736101, West Bengal, India
[3] Dept. of Mathematics, Jadavpur University, Kolkata 700032, West Bengal, India

Received: 11 December 2016
Published online: 28 February 2017 –

Abstract. The present paper investigates the effect of Stefan blowing on the hydro-magnetic bioconvection of a water-based nanofluid flow containing gyrotactic microorganisms through a permeable surface. Also we studied both actively and passively the controlled flux of nanoparticles and the effect of a surface slip at the wall. We adopt a similarity approach to reduce the leading partial differential equations into ordinary differential equations along with two separate boundary conditions (active and passive) and solve the resulting equations numerically by employing the RK-4 method through the shooting technique to perform the flow analysis. Discussions on the effect of emerging flow parameter on the flow characteristic are made properly through graphs and charts. We observed that the effects of the traditional Lewis number and suction/blowing parameter on temperature distribution and microorganism concentration are converse to each other. A fair result comparison of the present paper with formerly obtained results is given.

1 Introduction

Fluid particles movement caused heat transfer in the interior of fluid is known as convection, which occurs due to disparity among viscous and the buoyancy forces. Now bioconvection is a macroscopic self-transport by swimming of motile microorganisms like bacteria, algae or ciliated protozoa towards the upward direction. Since motile microorganisms are marginally denser in comparison with water and self-propelled, due to their gathering in suspensions, the upper surface becomes denser and unstable and the microorganisms fall down and consequently bioconvection started. Microorganisms always swim towards a specific direction due to the variation of externals stimuli. The movements in response to these stimuli are known as "taxes", including "chemotaxis" which implies the swimming due to chemical gradients, "phototaxis" which implies the movement along the direction of light or opposite to light, "gravitaxis" which implies the swimming under a gravitational field, "gyrotaxis" which implies the swimming due to the combination of two different torques: the first one is a viscous torque which acts upon a body placed in a shear flow and the second is a gravitational torque and "oxytaxis" which implies the swimming due to the oxygen gradient. The study of microorganisms and their behaviors is a crucial area of research work due to its considerable influence on human life. Microorganisms are generally used in chemical and food industries to produce medicine, everyday foods and insecticides and is also used in the breakdown of organic materials. A continuum model was proposed by Pedley *et al.* [1] for gyrotactic microorganism's suspensions and investigated the unstableness of the suspension. Utilizing this model Hill *et al.* [2] have drawn up a thorough study on the enhancement of the bioconvection pattern in a gyrotactic microorganisms suspension in a finite-depth layer. This model was further extended by Pedley and Kessler [3] who proposed a new model of bioconvection using the probability density function. Ghorai and Hill [4–7] made a research work based on that continuum model and extended it to their study on bioconvection in three dimension. Kuznetsov [8] studied the onset of the thermo-bioconvection of a suspension containing oxytactic bacteria. Recently Williams and Bees [9]

[a] e-mail: shibsankar.math@gmail.com
[b] e-mail: kd_kgec@rediffmail.com
[c] e-mail: kunduprabir@yahoo.co.in

discussed some important properties of the gyrotactic microorganisms by considering three different taxes. Srimani and Roopa [10] studied the effect of the rotation in gyrotactic bioconvection suspension. Srimani and Radha [11] observed the exterior magnetic field upshot on the chemotactic bacterial bioconvection and found a similarity solution.

A base fluid containing nanoparticles (1–50 mm) is identified as a nanofluid as defined by Choi [12]. Bioconvection within a nanofluid is now an emerging area for research work due to its major applications in biomicrosystem [13], biosensors [14], microdevices to measure the toxicity of nanoparticles [15]. For small nanoparticles concentration bioconvection occurs in a nanofluid, where nanoparticles do not increase the viscosity of the base fluid significantly. Nanoparticles are always not self-propelled and they move on due to Brownian motion and thermophoresis and are steered by the fluid flow. Studies on bioconvection with nanoparticles in suspension were first considered by Kuznetsov and Avramenko [16], after that several studies on nanofluid bioconvection have been carried out by many researcher [17–19]. Recently Khan *et al.* [20] scrutinized the MHD and Navier slip influence on nanofluids containing gyrotactic microorganisms. Mohyud-Din and Zaidi [21] discussed the Soret effect along with the MHD effect on the bioconvection with gyrotactic microorganisms. Das *et al.* [22] investigated the nanofluid bioconvection involving gyrotactic microorganisms together with chemical reactions and reported that the microorganisms concentration increases promoted with bioconvection Lewis number. Tausif *et al.* [23] discussed the multiple slip effects on the bioconvection in a nanofluid and established that the slip parameters and physical properties of the flow field are highly correlated. The solar radiation effect on bioconvection in a nanofluid was scrutinized by Acharya *et al.* [24]. After that Sarkar *et al.* [25] and Chakraborty *et al.* [26] made different studies on bioconvection in a nanofluid with gyrotactic microorganisms.

An assumption on nanoparticles concentration was given by Nield and Kuznetsov [27], which is the control of the nanoparticles concentration value that can be made by measuring the temperature at the boundary. Now the assumption of constant nanoparticles concentration at the surface is feasible by considering active control of the nanoparticles concentration area there. Latterly they assumed the problems [28–30] by considering newly setup boundary condition for nanoparticles concentration at the surface of the plate which is more realistic because that accounts for the effects of two parameters: the Brownian motion one together with the thermophoresis one. In the newly setup boundary condition the normal mass flux at the plate is zero and the nanoparticles concentration can be adjusted passively. The newly setup boundary condition among the applied inflictions has better agreement in nanofluids. After that by considering zero-mass nanoparticles flux at the wall several models have been presented by many researchers. Recently in different nanofluid problems many researcher used a revised model. Hayat *et al.* [31] used the zero-mass nanoparticle flux together with constant heat flux to find an optimal solution MHD nanofluid flow. Halim *et al.* [32,33] investigated the active and passive controls of nanoparticles on two different nanofluid flows, namely the Williamson and the Maxwell stagnation flow and in each case they agree with the fact that the temperature distribution in the passive case is less than the that in the active case. Atlas *et al.* [34] scrutinized the thermal radiation effect on the nanofluid flow among squeezed channels and at the lower surface described the analysis of active and passive controls of nanoparticles.

On the boundary layer blowing has a momentous role in nanoscience. Mass diffusion is determined by the flow field which is also affected by mass blowing at the wall. To give a correction in the conservation equations one can introduce the Stefan blowing factor at the wall. Fang and Jing [35] investigated the Stefan blowing effects on flow, heat and mass transfer and gave a solution in terms of the incomplete Gamma functions. Uddin *et al.* [36] discussed the Stefan blowing along with the multiple slip effects of bioconvection in a nanofluid involving microorganisms and employed Lie group of transformation to get similarity solution. An investigation on Stefan blowing together with multiple slip effects on gyrotactic nanofluid bioconvection was performed by Uddin *et al.* [37] who solved the similarity equations through employing the Chebyshev collocation method.

Motivated by the above-mentioned discussion in the present work we wish to investigate the effect of Stefan blowing of nanofluid bioconvection containing gyrotactic microorganism. Also we studied both actively and passively the control of nanoparticles at the wall. We adopted the similarity approach to reduce the leading partial differential equations into ordinary differential equations along with two separate boundary conditions (active and passive) and we solved the resulting equations numerically by employing the RK-4 method through the shooting technique to perform the flow analysis.

2 Mathematical analysis

We considered a water-based steady laminar electrically conducting flow of nanofluid containing gyrotactic microorganisms in a porous medium, in a two-dimensional structure. We consider the coordinate axes by taking the plate to be in the x-direction and the y-axis along the normal to the plate as depicted in fig. 1. We assume that the suspended nanoparticles are stable in the fluid and do not conglomerate. Also we assume that the microorganisms swimming direction and swimming velocity are not dependent on the appearance of nanoparticles and this hypothesis is vindicated if in the base fluid the concentration of nanoparticles is a lesser amount than 1% otherwise the bioconvection will be suppressed due to the presence of a greet viscosity of suspension. We assume the flow's magnetic Reynolds number is sufficiently small to neglect the induced magnetic field related to the corresponding applied magnetic field.

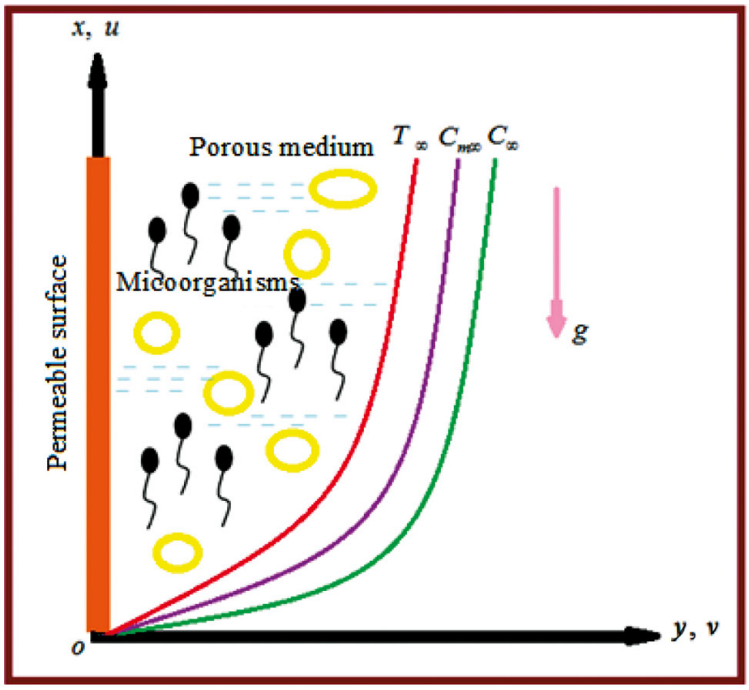

Fig. 1. Physical model and coordinate system.

Considering all the above assumptions along with the Oberbeck-Boussinesq approximation, the following equations for conservation of mass, momentum, thermal energy, nanoparticle concentration and microorganism density are formulated based upon the model mentioned by Khan *et al.* [20] as:

$$\frac{\partial u}{\partial x}+\frac{\partial u}{\partial y}=0, \tag{1}$$

$$\frac{\partial p}{\partial x}=u\frac{\partial^2 u}{\partial y^2}-\sigma B_0^2 u-\rho_f\left(u\frac{\partial u}{\partial x}+v\frac{\partial u}{\partial y}\right)-\frac{\varepsilon\mu}{k}u+g\left[(1-\varphi_\infty)\,\rho_{f\infty}\beta\,(T-T_\infty)-(\rho_p-\rho_{f\infty})\,(C-C_\infty)-C_m\gamma^*\,(\rho_{m\infty}-\rho_{f\infty})\right], \tag{2}$$

$$\frac{\partial p}{\partial y}=0, \tag{3}$$

$$u\frac{\partial T}{\partial x}+v\frac{\partial T}{\partial y}=\alpha\frac{\partial^2 T}{\partial y^2}+\tau\left\{D_B\frac{\partial C}{\partial y}\frac{\partial T}{\partial y}+\frac{D_T}{T_\infty}\left(\frac{\partial T}{\partial y}\right)^2\right\}, \tag{4}$$

$$u\frac{\partial C}{\partial x}+v\frac{\partial C}{\partial y}=D_B\frac{\partial^2 C}{\partial y^2}+\frac{D_T}{T_\infty}\frac{\partial^2 T}{\partial y^2}, \tag{5}$$

$$u\frac{\partial C_m}{\partial x}+v\frac{\partial C_m}{\partial y}+\frac{bW_c}{(C_w-C_\infty)}\left[\frac{\partial}{\partial y}\left(C_m\frac{\partial C}{\partial y}\right)\right]=D_m\frac{\partial^2 C_m}{\partial y^2}, \tag{6}$$

where u and v are, respectively, the velocity components in the x- and y-direction. Here T is the temperature, C the nanoparticle concentration, C_m the microorganism concentration, ε and k are, respectively, the porosity and permeability of the porous medium, μ stands for the viscosity of the nanofluid and microorganisms, σ is the electrical conductivity, B_0 the is magnitude of the applied transverse magnetic field, β the base fluid's volumetric coefficient of thermal expansion, γ^* the microorganism average volume, κ implies thermal conductivity, α is the nanofluid thermal diffusivity, $\tau=\frac{(\rho c_p)_s}{(\rho c_p)_f}$ is the ratio of the effective heat capacity among the nanoparticle material and the base fluid, ρ_f, ρ_m and ρ_p, respectively, stand for the base fluid density, the microorganism density and the nanoparticle density, D_B and D_T are, respectively, used for the coefficient of Brownian and thermophoretic diffusion, D_m is the microorganism diffusivity, W_c is the utmost cell swimming speed, the subscript ∞ is used for equivalent values at far field.

The appropriate boundary conditions designed for the present study are given by

$$u = N\frac{\partial u}{\partial y}, \quad v = -\frac{D_B}{1-C_w}\left(\frac{\partial C}{\partial y}\right), \quad T = T_w, \quad C_m = C_{mw}, \quad \text{at } y = 0,$$
$$\begin{cases} D_B\dfrac{\partial C}{\partial y} + \dfrac{D_T}{T_\infty}\dfrac{\partial T}{\partial y} = 0, & \text{for passive control of } \phi \\ C = C_w, & \text{for active control of } \phi \end{cases}, \quad \text{at } y = 0,$$
$$u \to 0, \quad v \to 0, \quad C \to C_\infty, \quad C_m \to C_{m\infty}, \quad \text{as } y \to \infty, \tag{7}$$

where N is the Navier slip coefficient, C_w, T_w, and $C_{m\infty}$ are, respectively, used for nanoparticles concentration, constant temperature and motile microorganism density at the wall.

Due to the small pressure gradient at the boundary, p has no momentous effect on the flow behaviors. Extracting p from (1) and (2) by applying cross-differentiation and using boundary conditions, we get

$$u\frac{\partial u}{\partial x} + v\frac{\partial u}{\partial y} = v_f\frac{\partial^2 u}{\partial y^2} - \frac{\sigma B_0^2}{\rho_f}u - \frac{\varepsilon v_f}{k}u + \left(\frac{1-\phi_\infty}{\rho_f}\right)\rho_{f\infty}\beta g\,(T - T_\infty) - \left(\frac{\rho_p - \rho_{f\infty}}{\rho_f}\right)g\,(C - C_\infty) - C_m g\gamma^*\left(\frac{\rho_{m\infty} - \rho_{f\infty}}{\rho_f}\right). \tag{8}$$

Introducing the non-dimensional functions $f(\eta)$, $\theta(\eta)$, $\phi(\eta)$, and $\chi(\eta)$ (η is the similarity variable) to convert eqs. (4)–(6) and (8) into ordinary differential equations as follows:

$$\eta = \frac{y}{x}Ra_x^{\frac{1}{4}}, \qquad \psi = \alpha Ra_x^{\frac{1}{4}}f(\eta), \qquad \theta(\eta) = \frac{T - T_\infty}{T_w - T_\infty}, \qquad \chi(\eta) = \frac{C_m - C_\infty}{C_{mw} - C_{m\infty}},$$
$$\phi(\eta) = \begin{cases} \dfrac{C - C_\infty}{C_\infty} & \text{for passive control of } \phi, \\ \dfrac{C - C_\infty}{C_W - C_\infty} & \text{for active control of } \phi, \end{cases} \tag{9}$$

where $Ra_x = \frac{(1-\phi_\infty)\beta g\Delta T_f}{\alpha v_f}x^3$ is the local Rayleigh number, the stream function $\psi(x, y)$ defined by $u = \frac{\partial \psi}{\partial y}$ and $v = -\frac{\partial \psi}{\partial x}$ also satisfies eq. (1). Using the substitution mentioned in eq. (9) into eqs. (4)–(6) and (8), we find the following similarity equations:

$$f''' + \frac{1}{4}\cdot \mathrm{Pr}^{-1}\left(3ff'' - 2f'^2\right) - Mf' + \theta - Br\phi - Rb\chi - Da^{-1}f' = 0, \tag{10}$$
$$\theta'' + \frac{3}{4}f\theta' + Nb\varphi'\theta' + Nt\theta'^2 = 0, \tag{11}$$
$$\phi'' + \frac{3}{4}Le\cdot f\phi' + \frac{Nt}{Nb}\cdot\theta'' = 0, \tag{12}$$
$$\chi'' + \frac{3}{4}Lb\cdot f\chi' - Pe\cdot\left[\phi'\chi' + \phi''\left(\sigma_b + \chi\right)\right] = 0. \tag{13}$$

Accordingly the boundary conditions (9) becomes

$$f(0) = \frac{4f_w\varphi'(0)}{3\mathrm{Le}}, \qquad f'(0) = \gamma f''(0), \qquad \theta(0) = 1, \qquad \chi(0) = 1,$$
$$\begin{cases} Nb\phi'(0) + Nt\theta'(0) = 0, & \text{for passive control of } \phi, \\ \phi(0) = 1, & \text{for active control of } \phi, \end{cases}$$
$$f'(\infty) = 0, \qquad \theta(\infty) = 0, \qquad \phi(\infty) = 0, \qquad \chi(\infty) = 0, \tag{14}$$

where the prime symbolizes ordinary differentiation with respect to η, $Lb = \frac{\alpha}{D_n}$ and $Le = \frac{\alpha}{D_B}$ are bioconvection and traditional Lewis number, respectively, $\sigma_b = \frac{C_{m\infty}}{\Delta C_{mw}}$ is the bioconvection constant, $Pe = \frac{bW_c}{D_m}$ and $Rb = \frac{\gamma^*\Delta C_{mw}\Delta\rho}{\rho_f(1-\phi_\infty)\beta\Delta T_w}$ are, respectively, the Peclet number and the Rayleigh number of bioconvection, $Br = \frac{(\rho_f - \rho_{f\infty})\Delta C_w}{\rho_f(1-\phi_\infty)\beta\Delta T_w}$ is the buoyancy ratio parameter,

$$Nb = \begin{cases} \dfrac{\tau D_B C_\infty}{\alpha}, & \text{for passive control of } \phi \\ \dfrac{\tau D_B \Delta C_w}{\alpha}, & \text{for active control of } \phi \end{cases} \quad \text{and} \quad Nt = \frac{\tau D_T \Delta T_w}{\alpha T_\infty}$$

Table 1. Comparison of $-\theta'(0)$ for different values of Pr.

Pr	Khan *et al.* [20]	Acharya *et al.* [24]	Das *et al.* [22]	Present result
1.0	0.40135	0.40145361	0.401452	0.40134232
10.0	0.46903	0.46931620	0.469315	0.46931621
100.0	0.49260	0.49252822	0.492529	0.49252835
1000.0	0.49878	0.49865112	0.498650	0.49865121

are, respectively, the Brownian motion and the thermophoresis parameter, $M = \frac{\sigma B_0^2 x^2}{\mu_f Ra_x^{\frac{1}{2}}}$ is the modified magnetic parameter, $C_T = \frac{T_\infty}{T_w - T_\infty}$ is the temperature ratio, $\mathrm{Pr} = \frac{v_f}{\alpha}$ and $Da^{-1} = \frac{\varepsilon x^2}{kRa_x^{\frac{1}{2}}}$ are, respectively, the Prandtl number and the inverse Darcy number, $\gamma = \frac{NRa_x^{\frac{1}{4}}}{x}$ is the velocity slip parameter, $f_w = \frac{\Delta C}{(1-C_w)}$ denotes the suction/blowing parameter.

3 Physical quantities

For engineering and practical purposes it is necessary to discuss various physically intended measures for instance Nusselt number (or wall heat transfer coefficient), Sherwood number (or wall deposition flux), density number of motile microorganisms (or rate of microorganism transfer). These are defined as

$$\begin{aligned} Nu_x &= -\frac{x}{(T_w - T_\infty)}\left(\frac{\partial T}{\partial y}\right)_{y=0}, \\ Sh_x &= -\frac{x}{(C_w - C_\infty)}\left(\frac{\partial C}{\partial y}\right)_{y=0}, \\ Nn_x &= -\frac{x}{(C_{mw} - C_{m\infty})}\left(\frac{\partial C_m}{\partial y}\right)_{y=0}. \end{aligned} \tag{15}$$

Using a non-dimensional variable we find that the reduced Nusselt number, the reduced Sherwood number and the reduced density number of motile microorganisms take the following forms:

$$\begin{aligned} Nu_r &= Ra_x^{-\frac{1}{4}} \cdot Nu_x = -\theta'(0), \\ Sh_r &= Ra_x^{-\frac{1}{4}} \cdot Sh_x = \begin{cases} -\dfrac{\phi'(0)}{\phi(0)}, & \text{for passive control of } \phi, \\ -\phi'(0), & \text{for active control of } \phi, \end{cases} \\ Nn_r &= Ra_x^{-\frac{1}{4}} \cdot Nn_x = -\chi'(0). \end{aligned} \tag{16}$$

4 Numerical procedure and code verification

Analytically it is impossible to find exact solution of the highly non-linear ordinary differential equations (10)–(13) subject to boundary conditions (14). We use Runge-Kutta-Fehlberg quadrature method through the shooting technique to resolve these equations with the prescribed boundary conditions in (14). Computations have been completed by employing the Maple-18 software. We replace $\eta \to \infty$ in boundary conditions by those at $\eta = \eta_\infty$. Inner iteration is done until we get the result up to desired accuracy 10^{-6} in all cases.

4.1 Testing of code

To test the exactness of numerical results and code employed in the present work we compared the different values of $-\theta'(0)$ for many values of the Prandtl number with identical presentation in different papers like Das *et al.* and Acharya *et al.* on non-appearance of nanofluid and bioconvection parameters with $Nt = Nb = Br = 10^{-5}$ and $Le = 10.0$. In table 1 we have arranged those values of $-\theta'(0)$ which are in excellent agreement with previous works which are mentioned above.

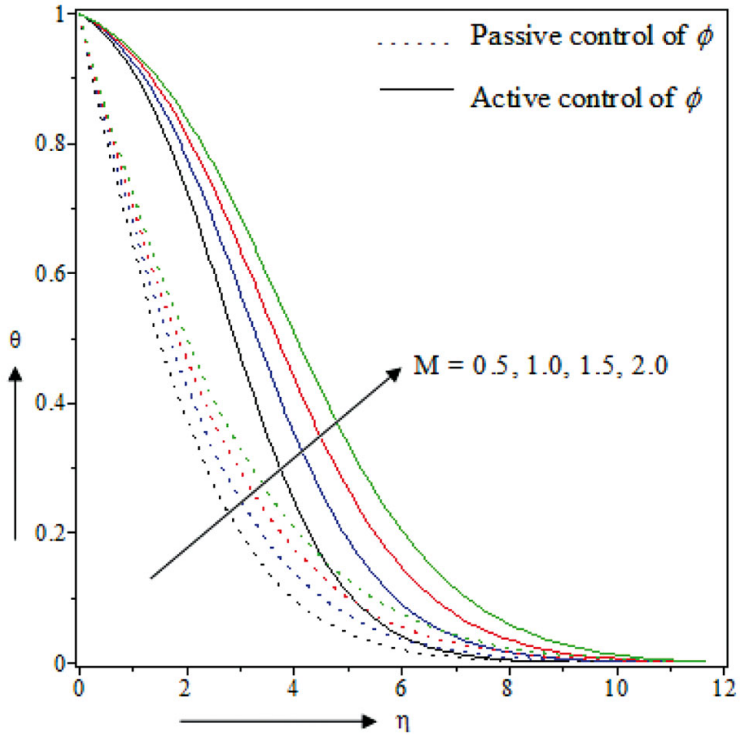

Fig. 2. Effect of the modified magnetic parameter M on the temperature distribution.

5 Result and discussions

The present work comprises the flow region's parametric study. We have epitomized the total discussion via tables and graphs to analyse the upshot of different emerging parameters, for instance, the modified magnetic parameter (M), traditional Lewis number (Le), suction/blowing parameters (f_w), bioconvection Lewis number (Lb), bioconvection Peclet number (Pe), bioconvection constant (σ_b). The default values of the emerging parameters during the simulation are taken as $M = 1.0$, $Br = 0.1$, $Rb = 0.3$, $Nb = 2.0$, $Nt = 1.0$, $Le = 1.0$, $Lb = 1.0$, $\sigma_b = 0.1$, $\lambda = 0.5$, $Pe = 1.0$, $f_w = 1.0$, $Da^{-1} = 0.5$ unless otherwise stated.

5.1 Effect of the modified magnetic parameter M

Figures 2–4, respectively, exhibit the impact of the modified magnetic parameter (M) on temperature, nanoparticle concentration and microorganism concentration against the similarity variable η. Figure 2 shows that the system of temperature distribution increases with M. Because when the power of M increases in an electrically conducting nanofluid it begins to produce a resistive force (Lorentz force) and nanoparticle erodes energy in the form of heat, consequently the boundary layer gets thicker. Figure 3 reveals that nanoparticle concentration profiles increase completely with M throughout the boundary layer for active control of ϕ, whereas for passive control of ϕ the nanoparticle concentration reduces for $0 \leq \eta \leq 3.5$ (approximately) and this is reverse for $\eta \geq 3.5$ (approximately). Figure 4 depicts that the microorganism concentration enhances with M throughout the boundary layer and hence its thickness increases. Notice that the temperature and nanoparticles concentration are higher in the case of active control of ϕ related to the same in the case of passive control of ϕ and the effect is opposite for microorganism concentration. When M increases then a reduction of Nu_r, Sh_r and Nn_r was observed in both cases, and this is tabulated in table 2 and table 3.

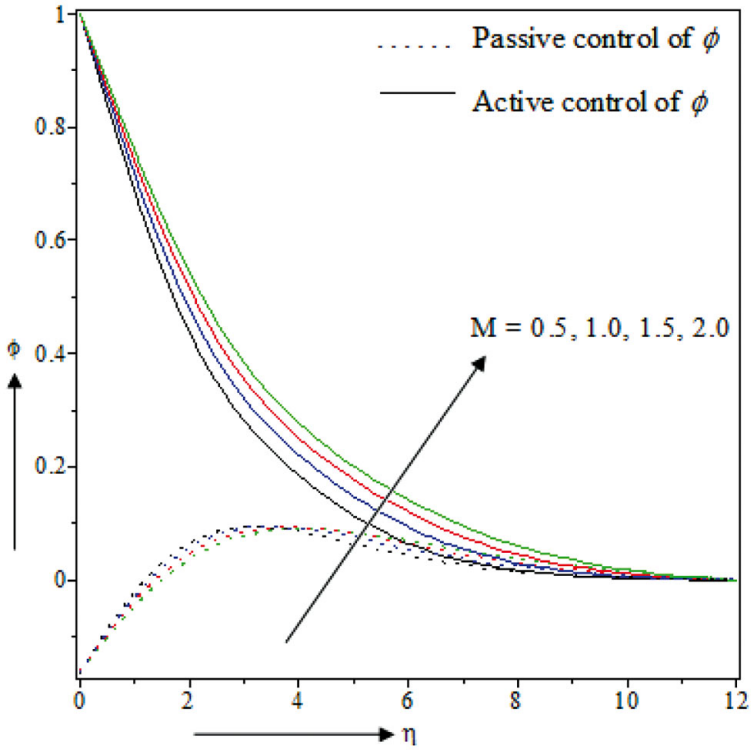

Fig. 3. Effect of the modified magnetic parameter M on the nanoparticles concentration.

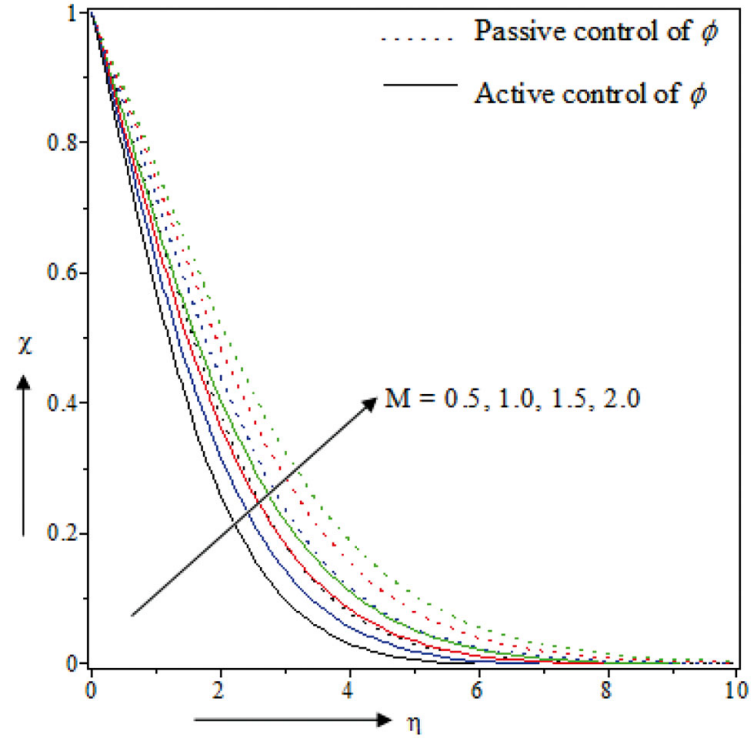

Fig. 4. Effect of the modified magnetic parameter M on the microorganism concentration.

Table 2. Numerical values of Nu_r, Sh_r for different values of M, Le and f_w.

M	Le	f_w	Nu_r		Sh_r	
			Active control	Passive control	Active control	Passive control
0.5			0.056164	0.399754	0.332520	0.986736
1.0			0.049926	0.356854	0.285038	0.909167
1.5			0.045147	0.325392	0.260944	0.839635
2.0			0.041307	0.301080	0.242086	0.776578
	0.8		0.050830	0.398935	0.249175	1.603183
	1.0		0.049926	0.356854	0.280316	1.423232
	1.2		0.049045	0.333893	0.307573	1.297592
	1.5		0.047888	0.313588	0.343346	1.211275
		0.5	0.061251	0.308996	0.415634	0.743116
		1.0	0.049926	0.356854	0.332520	0.989190
		1.5	0.042311	0.432813	0.280316	1.423232
		2.0	0.036813	0.585054	0.243919	2.354438

Table 3. Numerical values of Nn_r for different values of M, Le, f_w, Lb, Pe, σ_b.

M	Le	f_w	Lb	Pe	σ_b	Nn_r	
						Active control	Passive control
0.5						0.431472	0.286721
1.0						0.382754	0.256098
1.5						0.346900	0.233503
2.0						0.319220	0.215951
	0.8					0.345675	0.277051
	1.0					0.382754	0.256098
	1.2					0.414678	0.245422
	1.5					0.455805	0.236713
		0.5				0.489363	0.223057
		1.0				0.420067	0.241195
		1.5				0.382754	0.256098
		2.0				0.350746	0.274130
			0.8			0.376757	0.188127
			1.0			0.382754	0.256098
			1.2			0.385736	0.319778
			1.5			0.386323	0.409483
				1.0		0.377412	0.263430
				1.5		0.466561	0.185668
				2.0		0.563072	0.110735
				2.5		0.666132	0.038818
					0.0	0.226392	0.232992
					1.0	0.254692	0.198775
					1.5	0.268906	0.181806
					2.0	0.283159	0.164929

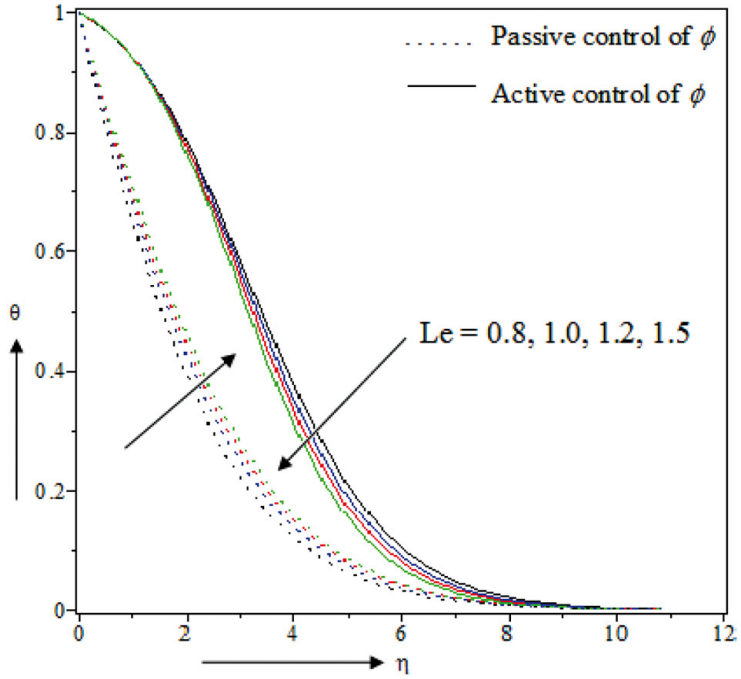

Fig. 5. Effect of the traditional Lewis number Le on the temperature distribution.

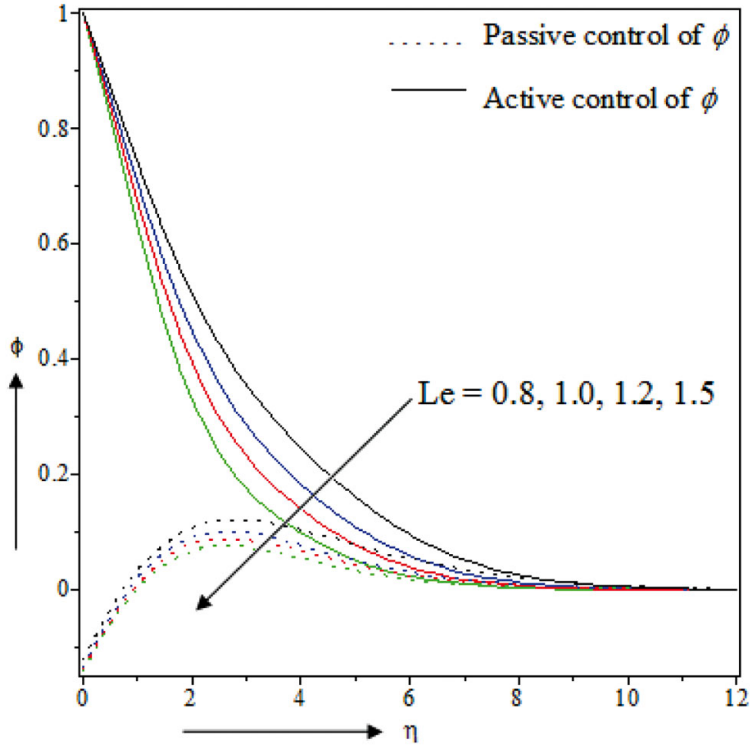

Fig. 6. Effect of the traditional Lewis number Le on the nanoparticles concentration.

5.2 Effect of the traditional Lewis number Le

The influence of the traditional Lewis number (Le) on temperature, nanoparticle concentration and microorganisms concentration is manifested in figs. 5–7, respectively. Figure 5 shows that in passive control the temperature distribution enhances with Le because Le is the ratio of thermal diffusion and Brownian diffusion parameter, and in passive control

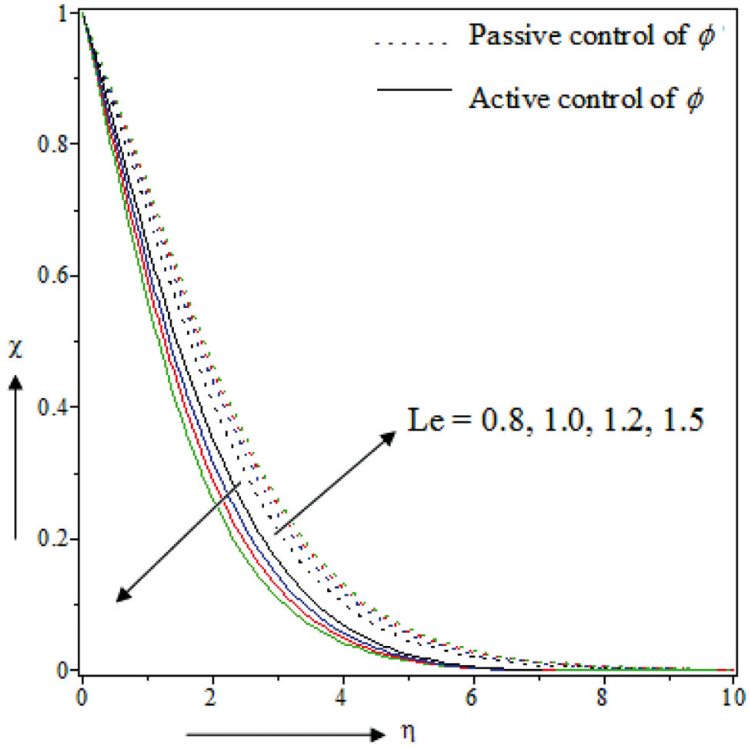

Fig. 7. Effect of the traditional Lewis number Le on the microorganism concentration.

the coefficient of Brownian diffusion is fixed at the least value and thermal diffusion most affects Le. Therefore an increase in Le implies that thermal diffusivity increases, consequently the temperature profiles are enriched but the result is reverse in active control. Also Nu_r decreases in each case with increasing Le as shown in table 2. Figure 6 illustrates that the nanoparticle concentration diminishes completely in the entire boundary layer with cumulative Le for each case. Since enhancing in Le implies decreasing in diffusion and hence reducing nanoparticle concentration. Figure 7 demonstrates that the microorganism concentration increases with Le in passive control whereas the opposite holds in active control. Sh_r and Nn_r increase with Le in active control but this is reverse for passive control.

5.3 Effect of the suction/blowing parameter f_w

Figures 8–10 show the typical profiles of non-dimensional temperature, nanoparticle concentration and microorganism concentration *versus* the similarity variable η, respectively. Figure 8 displays that in active control the temperature distribution increases with f_w whereas the opposite holds in passive control, it can also be seen that temperature profiles are higher in active control than in passive control. Figure 9 reveals that in active control nanoparticle concentration increases f_w in the entire boundary layer, whereas in passive control it increases for $0 \leq \eta \leq 3.8$ (approximately), it starts decreasing when $\eta \geq 3.8$ (approximately) and it asymptotically tends to zero as the distance from the boundary increases, it is also observed that the nanoparticle concentration profiles are lower in passive control than in active control. Figure 10 illustrates that the microorganism concentration reduces in passive control for cumulative f_w and the upshot is reversed in active control. The concentration profiles of microorganism in passive control are very high related to these in active control. In active control Nu_r, Sh_r and Nn_r all are regularly increasing with f_w and the respective values are decreasing in passive control.

5.4 Effect of the bioconvection Lewis number Lb

The impact of bioconvection Lewis number (Lb) on the concentration profiles of microorganisms is plotted in fig. 11. It shows the concentration profiles of the microorganisms reduces when Lb increases. A fact behind this is that the improvement of Lb implies a decrease of the microorganism diffusion, consequently the microorganism concentration reduces and hence the boundary layer becomes thinner. Also the concentration profiles of the microorganisms in passive control are higher with respect to those in active control. Nn_r increases with Lb in each case as tabulated in table 3.

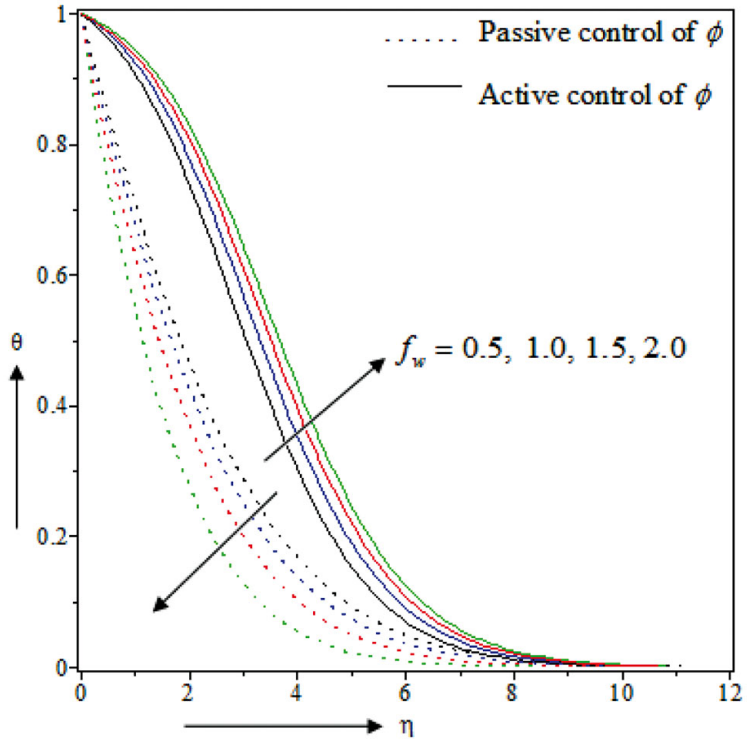

Fig. 8. Effect of the suction/blowing parameters (f_w) on the temperature distribution.

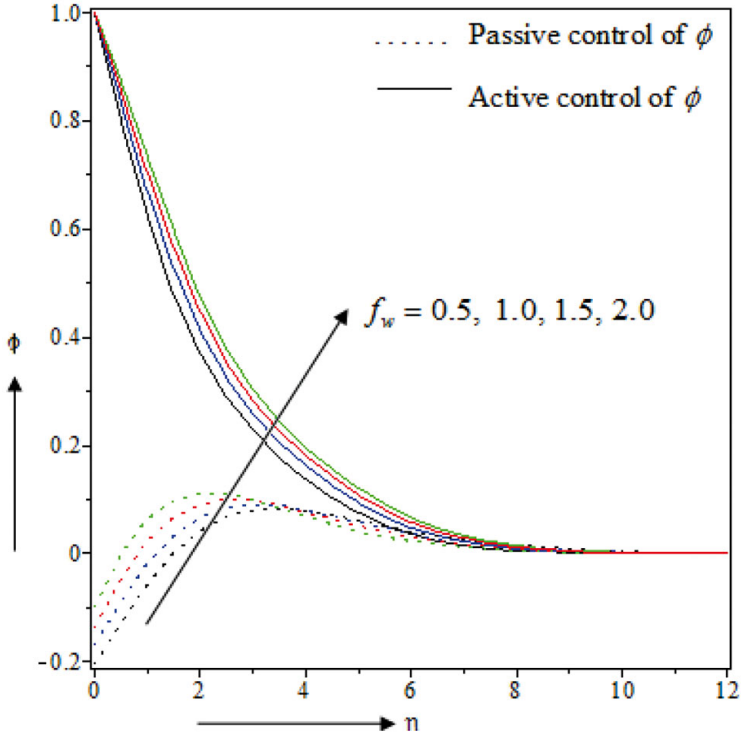

Fig. 9. Effect of the suction/blowing parameters (f_w) on the nanoparticles concentration.

5.5 Effect of the bioconvection Peclet number Pe and the bioconvection constant σ_b

Figures 12, 13, respectively, show the influence of the bioconvection Peclet number (Pe), bioconvection constant (σ_b) on the microorganism concentration. Figure 12 reveals that in active control when Pe increases the microorganism concentration lowers and asymptotically tends to zero as the distance from the boundary increases and the outcome is

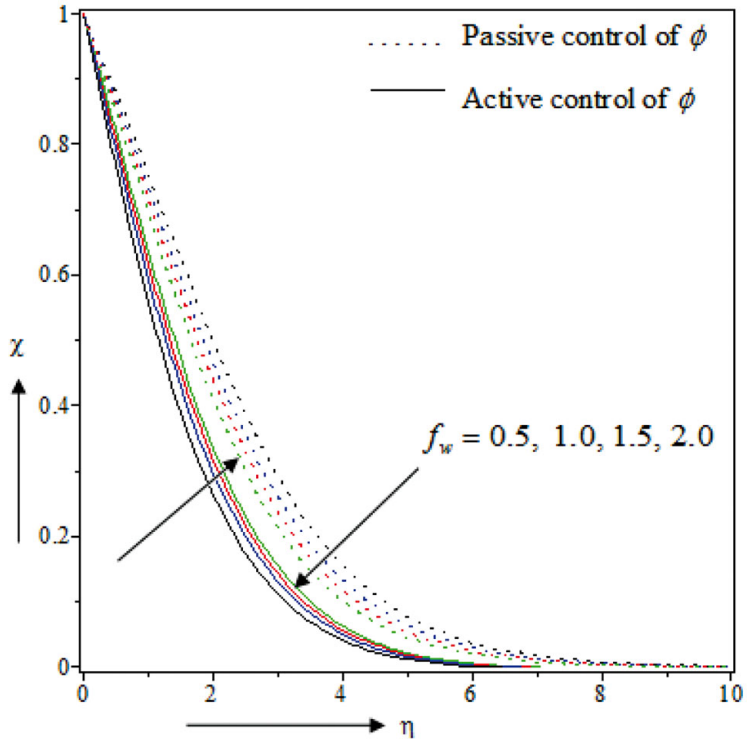

Fig. 10. Effect of the suction/blowing parameters (f_w) on the microorganism concentration.

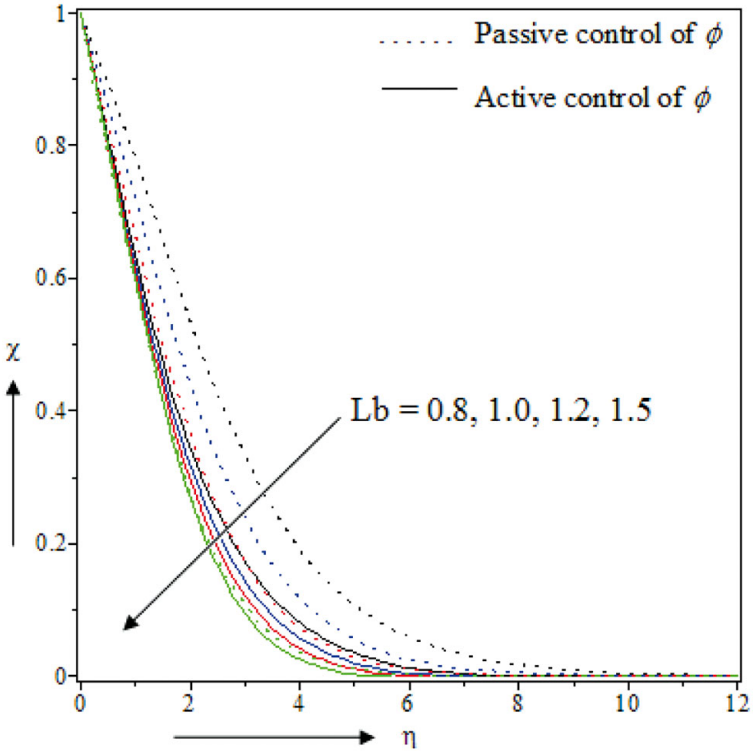

Fig. 11. Effect of the bioconvection Lewis number Lb on the microorganism concentration.

the opposite in passive control. It is also found that concentration profiles in passive control are higher than those in active control. The impact of σ_b on the microorganism concentration profiles identically agrees with the concentration profiles of Pe as displayed in fig. 13. In passive control Nn_r reduces with the strong enhancement of Pe and σ_b, but we found opposite results in active control.

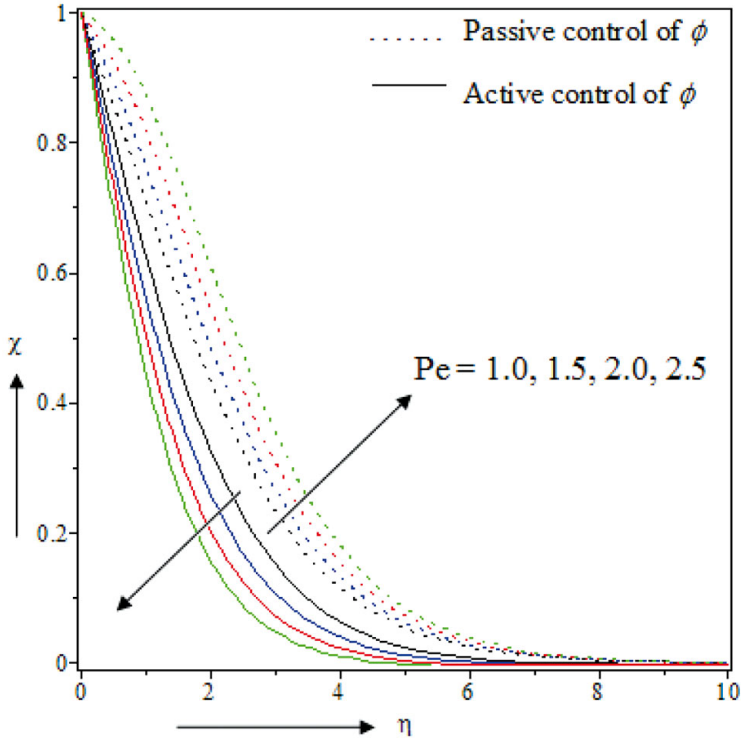

Fig. 12. Effect of the bioconvection Peclet number Pe on the microorganism concentration.

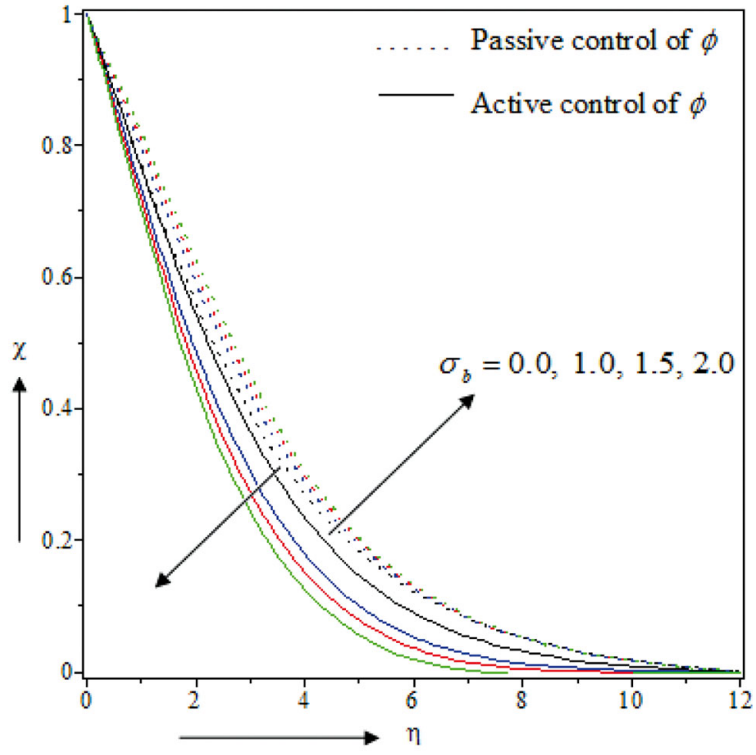

Fig. 13. Effect of the bioconvection constant (σ_b) on the microorganism concentration.

6 Conclusions

In the present work we developed the influence of active and passive boundary condition at the plate (wall) and the Stefan blowing effects on a water-based steady laminar electrically conducting flow of nanofluid including gyrotactic microorganisms in a porous medium in a two-dimensional structure. The transformed ordinary differential equations were derived from the leading partial differential equations through employing the similarity transformation.

We use the Runge-Kutta-Fehlberg quadrature method through shooting technique to solve these equations with the prescribed boundary conditions and illustrate the impact of the various emerging parameters on the entire nanofluid flow. In our discussion we found many results among which very specific conclusions are listed below:

- The effects of Le and f_w on temperature distribution and microorganism concentration are opposite to each other.
- The temperature profiles in active control are higher than those in passive control for M, Le, f_w.
- The impacts of σ_b and Pe on the microorganism concentration profiles are identical.
- In active control the microorganism concentration profiles are less than those in passive control for M, Le, f_w, Lb, Pe, σ_b.
- The nanoparticles concentration increases entirely in boundary layer with M, f_w and decreases when Le increases. Also the nanoparticles concentration is higher in active control than in passive control for all cases.
- Nu_r, Sh_r and Nn_r reduce when M increases for each case. Nu_r, Sh_r and Nn_r have the opposite effect for f_w in active and passive boundary conditions.

The authors wish to express their cordial thanks to reviewers for valuable suggestions and comments to improve the presentation of this article. Finally, the authors wish to express their sincere thanks to the Editors-in-Chief and the Production Office for primary consideration and correcting the mistakes for publication in *The European Physical Journal Plus*.

References

1. T. Pedley, N.A. Hill, J.O. Kessler, J. Fluid Mech. **195**, 223 (1988).
2. N.A. Hill, T. Pedley, J.O. Kessler, J. Fluid Mech. **208**, 509 (1989).
3. T. Pedley, J.O. Kessler, J. Fluid Mech. **212**, 155 (1990).
4. S. Ghorai, N.A. Hill, J. Fluid Mech. **400**, 1 (1999).
5. S. Ghorai, N.A. Hill, Bull. Math. Biol. **62**, 429 (2000).
6. S. Ghorai, N.A. Hill, J. Theor. Biol. **219**, 137 (2002).
7. S. Ghorai, N.A. Hill, Phys. Fluids **19**, 054107 (2007).
8. A.V. Kuznetsov, Int. Commun. Heat Mass Transfer **32**, 991 (2005).
9. C.R. Williams, M.A. Bees, J. Exp. Biol. **214**, 2398 (2011).
10. P.K. Srimani, M.C. Roopa, Int. J. Curr. Res. **3**, 114 (2011).
11. P.K. Srimani, D. Radha, Int. J. Appl. Math. Stat. Sci. **2**, 27 (2013).
12. S.U.S. Choi, *Developments and Application of Non-Newtonian Flows* (ASME Press, New York, USA, 1995).
13. T. Tsai, D. Liou, L. Kuo, P. Chen, Sensors Actuat. A Phys. **153**, 267 (2009).
14. H. Li, S. Liu, Z. Dai, J. Bao, Sensors **9**, 8547 (2009).
15. A. Munir, J. Wang, H.S. Zhou, IET Nanobiotechnol. **3**, 55 (2009).
16. A.V. Kuznetsov, A.A. Avramenko, Int. Commun. Heat Mass Transfer **31**, 1 (2004).
17. A.V. Kuznetsov, P. Geng, Int. J. Numer. Methods Heat Fluid Flow **15**, 328 (2005).
18. A.V. Kuznetsov, Int. Commun Heat Mass Transfer **37**, 1421 (2010).
19. A.V. Kuznetsov, Nanoscale Res. Lett. **6**, 100 (2011).
20. W.A. Khan, O.D. Makinde, Z.H. Khan, Int. J. Heat Mass Transfer **74**, 285 (2014).
21. S.T. Mohyud-Din, Syed Zulfiqar Ali Zaidi, Neural Comput. Appl. (2016) DOI: 10.1007/s00521-016-2366-9.
22. K. Das, P.R. Duari, P.K. Kundu, J. Mech. Sci. Technol. **29**, 1 (2015).
23. Md.T. Sk, K. Das, P.K. Kundu, J. Mol. Liq. **220**, 518 (2016).
24. N. Acharya, K. Das, P.K. Kundu, J. Mol. Liq. **222**, 28 (2016).
25. A. Sarkar, K. Das, P.K. Kundu, J. Mol. Liq. **223**, 725 (2016).
26. T. chakraborty, K. Das, P.K. Kundu, Alex. Eng. J. (2016) DOI: 10.1016/j.aej.2016.11.011.
27. D.A. Nield, A.V. Kuznetsov, Int. J. Heat Mass Transfer **52**, 5792 (2009).
28. D.A. Nield, A.V. Kuznetsov, Int. J. Heat Mass Transfer **65**, 682 (2013).
29. D.A. Nield, A.V. Kuznetsov, Int. J. Heat Mass Transfer **77**, 915 (2014).
30. D.A. Nield, A.V. Kuznetsov, Int. J. Heat Mass Transfer **68**, 211 (2014).
31. T. Hayat, Z. Hussain, A. Alsaedi, T. Muhammad, Neural Comput. Appl. (2016) DOI: 10.1007/s00521-016-2685-x.
32. N.A. Halim, S. Sivasankaran, N.F.M. Noor, Neural Comput. Appl. (2016) DOI: 10.1007/s00521-016-2380-y.
33. N.A. Halim, R.U. Haq, N.F.M. Noor, *Meccanica* (2016) DOI: 10.1007/s11012-016-0517-9.
34. M. Atlas, R.U. Haq, T. Mekkaoui, J. Mol. Liq. **223**, 289 (2016).
35. T. Fang, W. Jing, Commun Nonlinear Sci. Numer. Simulat. **19**, 3086 (2014).
36. Md. J. Uddin, M.N. Kabir, O.A. Beg, Int. J. Heat Mass Transfer **95**, 116 (2016).
37. Md. J. Uddin, Y. Alginahi, Md. J. Uddin, M.N. Kabir, Comput. Math. Appl. **72**, 2562 (2016).